23rd ABCM International Congress of Mechanical Engineering
December 6-11, 2015, Rio de Janeiro, RJ, Brazil

PARAMETRIC ANALYSIS OF PARTICULATE FLOW FOR FLUID LOSS CONTROL APPLIED TO SEALING FRACTURED CHANNELS

Marcos Vinicius Barbosa
Fernando César De Lai
Admilson T. Franco
Silvio L. M. Junqueira
Research Center for Rheology and Non-Newtonian Fluids (CERNN), Postgraduate Program in Mechanical and Materials Engineering (PPGEM), Federal University of Technology - Paraná (UTFPR) - Av. Sete de Setembro, 3165, CEP 80.230-901 - Curitiba-PR-Brazil
marcoscp2@gmail.com, fernandodelai@utfpr.edu.br, admilson@utfpr.edu.br, silvio@utfpr.edu.br

Abstract. *The aim of this work is numerically investigate the particulate flow applied to filling fractures in formations during the drilling operation. Regarding the analysis procedure, the study is divided into two parts: the first one is the analysis of the fluid loss due to the presence of a fracture in a channel (which is treated as a single-phase flow); and the second part concerns the two-phase liquid-solid flow to investigate the filling process of a discrete fracture. The particulate flow is studied via a numerical model applying an Eulerian-Lagrangian approach. The coupling between the phases is achieved by the Dense Discrete Phase Model (DDPM) and the Discrete Element Method (DEM) is used to account for the particles collisions. The fracture filling process is analyzed by the flow's Reynolds number and by the particle to fluid density ratio. The results are presented, mainly, through the bed length, height, position inside the fracture and how such parameters can be related to the maximum reduction of the fluid loss in the least time possible. In order to avoid fracturing the formation during the injection process, the pressure on the channel inlet is also monitored to guarantee that the fracturing pressure is not surpassed by the buildup pressure generated by the particles injection.*

Keywords: *particulate flow, fractured channel, fluid loss, DDPM-DEM*

1. INTRODUCTION

Defined as the mud flow from the wellbore to the formation, the lost circulation phenomenon is a major problem in the oil and gas industry. It is estimated that the impact of lost circulation during the well construction phase accounts for US$ 2 to 4 billion annually in losses of time, drilling fluid and materials used to stem the losses (Cook *et al.*, 2012).

To observe the lost circulation phenomenon, the pressure on the wellbore has to be higher than the pore pressure of the formation (Tiab and Donaldson, 2004). When this occur, the fluid may escape through the existing pores on the formation impacting solid removal, bit refrigeration and wellbore stability.

Also, the phenomenon may be intensified if fractures are present in the formation. Usually, during the drilling operation, fractures may be present by two mechanisms: one caused by the drilling operation itself, when the pressure inside the wellbore (calculated from the equivalent mud weight - EMW) surpasses the fracture pressure of the formation; and another by drilling a naturally fractured reservoir (Tiab and Donaldson, 2004).

When the lost circulation occurs associated with the presence of a fracture, one of the techniques used to remediate the problem consists in adding particulate material with selected granulometry, called Lost Circulation Materials (LCM) to the mud (Suyan *et al.*, 2007). It is expected that the particles will be carried by the mud flow throughout the whole fractured channel, including the fracture itself. When reaching the fracture region, the particles will deposit inside the fracture and form a bed, which will reduce or eliminate the mud flow towards the formation.

The particle addition to the mud may be employed in two scenarios: with or without the suspension of the drilling process. When the drilling operation is stopped, the column is removed up to the point in which the fracture is located and the LCM are added to the mud. This operation has two major downsides: the difficulty of locating the fracture (which was recently studied by Chen *et al.* (2014)); and the possibility of promoting a kick, which is the fluid flow from the formation towards the well (Crespo and Ahmed, 2013).

The second approach consists in adding the particles to the mud and promote the so called plugging while drilliing (Peng *et al.*, 1996). This technique has been recently studied by De Lai (2013) and Barbosa (2015) and poses an effective way of promote the reduction of the fluid loss due to the presence of a fracture.

When promoting the sealing of a fracture using lost circulation materials, there are several mechanisms that may influence the particle bed formation inside the fracture that can be grouped in three classes: geometric parameters of the fracture, flow parameters and injection parameters. Geometric parameter of the fracture include the fracture length and aperture (thickness); flow parameters comprise the flow's Reynolds number and the fluid properties (such as viscosity and density); injection parameters consists of the particles diameter, the amount of particles injected into the mud and the particle to fluid density ratio.

In this work, an analysis of the influence of the Reynolds number and the particle to fluid density ratio is performed. The main results are presented using the fluid loss along the time (Q_{loss}), the monitoring of the pressure in the fractured channel inlet (P_{inlet}) and the total time of the filling process (t_{fill}). The main parameters regarding the particle bed, such as the bed initial position inside the fracture ($h_{i,pct}$), bed length (h_{pct}) and the vertical filling of the fracture ($e_{pct,\%}$) are also presented.

2. PROBLEM CHARACTERIZATION

The operations in the oil and gas industry are quite complex. Therefore, describing the geometry and operating conditions of a wellbore in a complete form is a rather difficult task to accomplish. In order to make possible to analyze the problem in an effective way, simplifications and assumptions have to be done.

The first set of assumptions regards the geometry. Usually, the wellbore is considered in a vertical position and the fracture has a geometry that is irregular throughout its length, the formation presents a porous-like structure and the annulus is defined as the space between the perforation column and the formation.

The geometry used in this work considers: (1) a well defined geometry for the fracture; (2) an impermeable interface between the formation and the annulus; (3) a rectangular section of the fractured channel. Figure 1(a) shows an axial cut on the simplified wellbore set using the aforementioned mentioned simplifications.

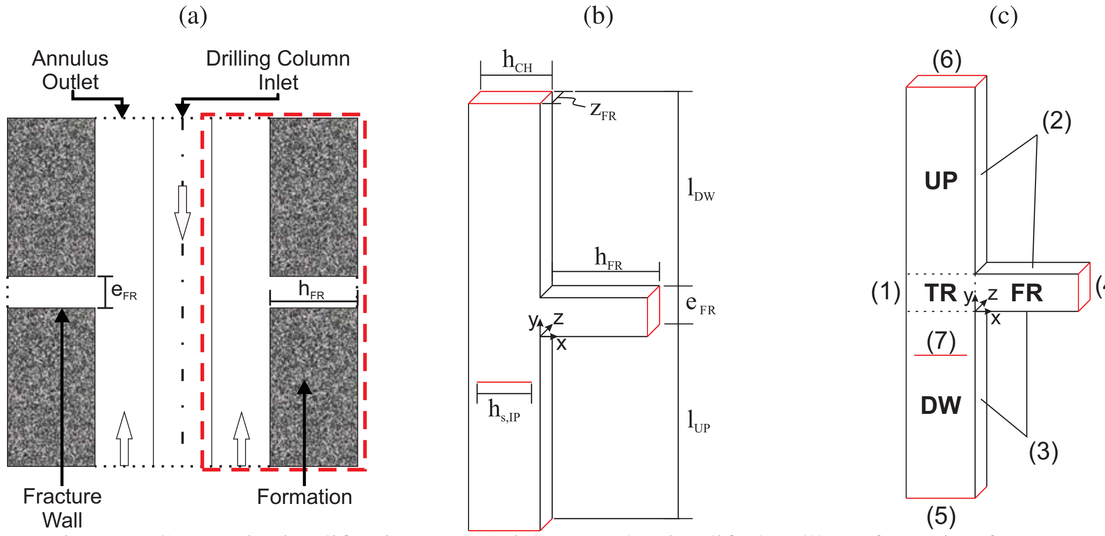

Figure 1: Geometric simplifications: (a) Axial cut on the simplified wellbore-formation-fracture set and (b) Three-dimensional computational geometry

Note that the symmetry plane shown in Fig. 1(a) which can be used to reduce computational costs. As described before, the region of interest in this work comprehends the annulus and the fracture itself, as the aim is to observe the particle transport from the annulus to the fracture, as highlighted in Fig. 1(a). By using the discussed considerations, the final computational domain used in this work can be seen in Fig. 1(b).

The fractured channel geometry shown in Fig. 1(b), consists in the annulus with a h_{CH} thickness and a length that is a sum of the upstream length (l_{UP}), downstream length (l_{DW}) and the fracture thickness (e_{FR}). The fracture is defined by its thickness and length (h_{FR}). The whole wellbore-fracture set has a third dimensional component z_{FR} to treat the particle deposition as a 3D problem. The surface on which the particle injection will be made has a length $h_{s,IP}$.

The problem has four regions of interest, showed in Fig. 1(c): the downstream region **DW**, which is the region where the particles are injected through the particle injection surface (7); the transition region **TR**, where the particles start to be carried from the channel to the fracture and; the upstream region **UP**, representing the returning of the flow towards the wellbore head and; the fracture region **FR** where the particles will deposit. Still in Fig. 1(c), the surfaces (1), (2) and (3) represent impermeable surfaces and surfaces (4), (5) and (6) are the fracture outlet, channel inlet and outlet, respectively.

As mentioned earlier, the fluid loss occurs due to the pressure configuration in the borehole so that the correct description of such conditions is a key point for a successful numerical simulation. One clever way to set the pressure in the numerical domain was introduced by De Lai (2013). The author proposed dividing the lost circulation problem and the particle injection process into three subproblems: (1) lost circulation problem with prescribed mass flux, (2) lost circulation problem with precribed pressures and (3) the particle injection process.

The subproblem (1) - lost circulation phenomenon with prescribed mass flux consists in setting the percentage of fluid being lost due to the presence of the fracture (Q_{loss}). As consequence, only a fraction of the initial fluid being injected in the channel will return through the channel outlet, given by $Q_{\beta,CH,o}$. The boundary condition for the surface (1) (channel inlet) is defined as a prescribed velocity $U_{\beta,CH,i}$ obtained from the flow's Reynolds number, as shown in Eq. (1). Also, for surfaces (1), (2) and (3), all considered impermeable, the non-slip condition is applied.

$$U_{\beta,CH,i} = \frac{Re\mu_\beta}{\rho_\beta h_{CH}} \tag{1}$$

where Re is the flow Reynolds number, μ_β and ρ_β represent the fluid viscosity and density, respectively.

Once a fully developed flow is achieved in the subproblem (1), both the fracture and channel outlet pressures are obtained and used as a new set of boundary conditions for the subproblem (2).

The invasion problem with prescribed pressure, subproblem (2), uses the pressure condition obtained from the subproblem (1) to mimic the pressure condition in a borehole during the fluid loss phenomenon. It is a rather clever maneuver applied to describe such difficult conditions, since it takes in to account the percentage of fluid being lost due to the presence of a fracture. Again, after a fully developed flow is achieved, the particle injection process takes place.

The particle injection, subproblem (3), consists in releasing a stream of particles (surface (7) in Fig. 1(a)) that will be carried in the annulus region to the fracture region in order to fill up the fracture and eliminate or reduce the initial fluid loss. The particles are released in the particle injection surface - surface (7) in Fig. 1(c).

3. NUMERICAL MODEL

To describe the coupling of the fluid and solid phases, the Dense Discrete Phase Model (DDPM), proposed by Popoff and Braun (2007), is applied. This model was chosen due to its capability to represent both, dilute and dense flow. Usually, a dilute flow is observed in the annulus region and, due to the packing of particles over time, dense flow is observed along the fracture.

The model accounts for two sets of equations: one for the fluid and another for the particles. The fluid is modeled as a continuum and the mass and momentum conservation are applied, as shown in Eq. (2) and Eq. (3), respectively.

$$\frac{\partial \epsilon_\beta \rho_\beta}{\partial t} + \nabla \cdot (\epsilon_\beta \rho_\beta \mathbf{u}_\beta) = 0 \tag{2}$$

$$\frac{\partial (\epsilon_\beta \rho_\beta \mathbf{u}_\beta)}{\partial t} + \nabla \cdot (\epsilon_\beta \rho_\beta \mathbf{u}_\beta \mathbf{u}_\beta) = -\epsilon_\beta \nabla \mathbf{p}_\beta + \nabla \cdot (\epsilon_\beta \mu_\beta \nabla \cdot \mathbf{u}_\beta) + \epsilon_\beta \rho_\beta \mathbf{g} + \mathbf{F}_{DPM} + \mathbf{S}_{DPM} \tag{3}$$

in which ϵ_β, ρ_β, μ_β represent the fluid volume fraction, density and absolute viscosity, respectively. $\mathbf{u}_\beta$ is the fluid velocity $\mathbf{u}_\beta$ $\mathbf{p}_\beta$ is the fluid pressure. Gravity acceleration is indicated by $\mathbf{g}$ and time is represented by t. The coupling force between the phases is represented by $\mathbf{F}_{DPM}$ and the source term S_{DPM} is included to account for the displacement of fluid due to a particle entering in a control volume.

The velocity equation, Eq. (4), and Newton's Second Law of Motion, Eq. (5) are applied in order to track the particles individually throughout the numerical domain.

$$\frac{d\mathbf{x}_p}{dt} = \mathbf{u}_p \tag{4}$$

$$m_p \frac{d\mathbf{u}_p}{dt} = \mathbf{F}_D + \mathbf{F}_{gb} + \mathbf{F}_{pg} + \mathbf{F}_{vm} + \mathbf{F}_{sl} + \mathbf{F}_{DEM} \tag{5}$$

In Eq. (4) and Eq. (5), $\mathbf{x}_p$, $\mathbf{u}_p$ and m_p represent the particle position, velocity and mass, respectively. The drag force, gravity and buoyancy forces, pressure gradient force, virtual mass and Saffman's lift forces are indicated by $\mathbf{F}_D$, $\mathbf{F}_{gb}$, $\mathbf{F}_{pg}$, $\mathbf{F}_{vm}$, $\mathbf{F}_{sl}$, respectively. The collision force among the particles is indicated by $\mathbf{F}_{DEM}$. Table 1 summarizes the aforementioned forces.

In Table 1, ρ_p stands for the particle density and Re_p is the particle's Reynolds number given by $Re = \rho_\beta |\mathbf{u}_\beta - \mathbf{u}_p| D_p/\mu_\beta$. C_D represents the drag coefficient, obtained from Morsi and Alexander (1972), C_{sl} is the Saffman's constant (Li and Ahmadi (1992)) and C_{vm} the virtual mass coefficient as defined by Kendoush *et al.* (2007).

The $\mathbf{F}_{DEM}$ term is a combination of normal and tangential forces, so that $\mathbf{F}_{DEM} = \mathbf{F}_n + \mathbf{F}_t$. The normal force is calculated using a spring-dashpot model, Luding (1998), in which the collision force is described using a stiffness constant

Table 1: Forces acting upon a solid particle

Force		Equation
Gravitational and Buoyance		$\mathbf{F}_{gb} = m_p \frac{\rho_p - \rho_\beta}{\rho_p}\mathbf{g}$
Pressure gradient		$\mathbf{F}_{pg} = m_p \frac{\rho_\beta}{\rho_p}(\mathbf{u}_\beta \nabla \cdot \mathbf{u}_\beta)$
Virtual mass		$\mathbf{F}_{vm} = C_{vm} m_p \frac{\rho_\beta}{\rho_p}\frac{D}{Dt}(\mathbf{u}_\beta - \mathbf{u}_p)$
Drag force		$\mathbf{F}_D = \frac{3}{4}\frac{m_p \mu_\beta}{\rho_p D_p^2} C_D Re_p (\mathbf{u}_\beta - \mathbf{u}_p)$
Saffman's lift		$\mathbf{F}_{sl} = C_{sl} m_p \frac{\rho_\beta}{\rho_p}(\nabla \times \mathbf{u}_\beta) \times (\mathbf{u}_\beta - \mathbf{u}_p)$
Colision Forces	Normal	$\mathbf{F}_n = [k\delta + \gamma \mathbf{u}_{12} \cdot \boldsymbol{\lambda}_{12}]\boldsymbol{\lambda}_{12}$
	Tangential	$\mathbf{F}_t = -\mu_a |\mathbf{F}_n| \boldsymbol{\zeta}_{12}$

k and a damping coefficient γ, based on a restitution coefficient η, as shown in Eq. 6. To calculate the normal force, as shown in Tab. 1, it is necessary to determine the particle superposition δ for the collision, the relative velocity $\mathbf{u}_{12}$ and the normal direction of the collision λ_{12}.

$$\gamma = -\frac{m_{12}}{t_{col}} ln(\eta) \tag{6}$$

The tangential force $\mathbf{F}_t$ is calculated using a Coulumb friction model as discussed in Luding (1998). In order to do so, the model is based on a friction coefficient μ_a and the tangential direction $\boldsymbol{\zeta}_{12}$.

4. RESULTS AND DISCUSSION

First, an analysis of the influence of the flow's Reynolds number is presented with a $Q_{loss} = 10\%$. All the simulations were perfomed using a mesh of 19600 volumes. The fluid and particle time step sizes are $2 \cdot 10^{-2}$ and $2 \cdot 10^{-4}$, respectively. The fracture channel has dimensions of $l_{UP} = 1.800\ m$, $l_{DW} = 0.225\ m$ and $h_{CH} = 0.045\ m$. The fracture has a length $h_{FR} = 0.720\ m$ and thickness $e_{FR} = 0.010\ m$. The fluid has a density of $\rho_\beta = 1187.6\ kg/m^3$ and an absolute viscosity of $\mu_\beta = 27.973 \cdot 10^{-3}\ Pa \cdot s$. For the lost circulation analysis, configurations with Reynolds number of $Re = 250$, 500 and 750 were investigated.

The results for the lost circulation phenomenon are shown in Fig. 2 and are presented using the velocity and pressure fields. As can be seen, increasing the flow's Reynolds number causes an increase on the recirculation zone in the fracture inlet. Also, the maximum velocity attained in the fracture inlet, right above the recirculation zone, increases as a result of the expansion on the recirculation zone.

According to the pressure field shown in Fig. 2, there is an increase in the pressure on the fracture inlet region, as the Reynolds numbers is augmented. The combination of the velocity and pressure in the fracture inlet region may contribute to the fracture filling, since it facilitates the particle transport in that region.

The particle packing process is affected by several parameters: the fluid loss (Q_{loss}), the Reynolds number (Re) and the fluid viscosity (μ_β) for the flow parameters; the injection parameters are the particle diameter (D_p), the particle to fluid density ratio ($\rho_{p/\beta}$), the amount of particle being injected ($N_{p,inj}$) on the injection and the frequency of injection Δt_{inj}; the geometric characteristics of the fracture such as the fracture thickness e_{FR} and length h_{FR} also shows influence on the particle packing inside the fracture. All these parameters have been recently investigated by De Lai (2013) e Barbosa (2015).

As can be seen, there are a large amount of variables that can affect the filling process of a fracture. As it have been already analyzed from the fluid loss point of view, the influence of the Reynolds number (Re) over particle packing is also studied in the fracture filling process. Moreover, the particle to fluid density ratio ($\rho_{p/\beta}$) is analyzed as well.

In the Reynolds number analysis, it is considered a particle with $D_p = 0.5\ mm$, $\rho_{p/\beta} = 2.25\ kg/m^3$ and 30 particles are injected simultaneously in the flow.

The result for the particle packing inside the fracture is displayed in Fig. 3. Take notice that the initial position of the bed $h_{pct,i}$ has a strong dependency on the flow's Reynolds number. As Re increases, the particle bed tends to be formed far from the fracture inlet, gaining length (h_{pct}) and losing its capacity of vertically fill the fracture ($e_{FR,\%}$), confirmed in Tab. 2.

Since the injection process is the same for the three Reynolds numbers the difference in the position of the bed can

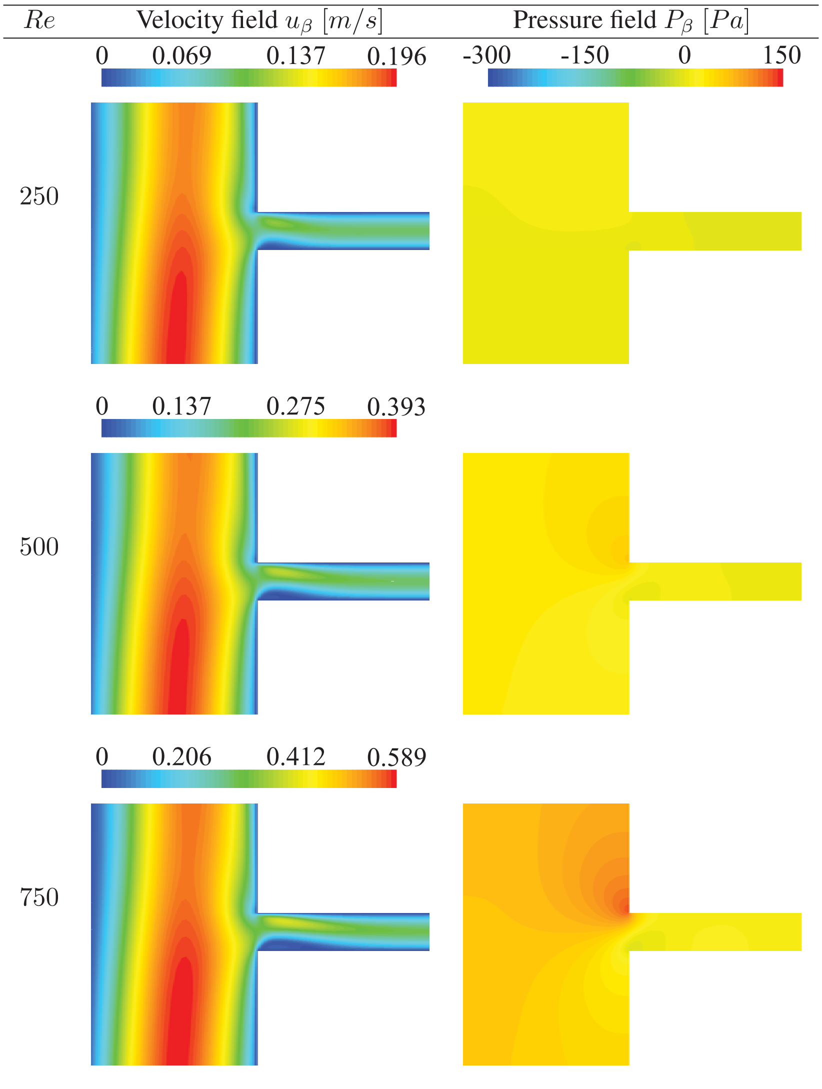

Figure 2: Velocity and Pressure field for several Reynolds number. The fluid loss for all configurations is set as $Q_{loss} = 10\%$.

be explained by the intrinsic change on the ability of the flow to carry the particles: for higher Reynolds numbers, the flow has more energy to transport the particles which causes the bed length to increase, difficulting the particle's vertical packing.

Defined as the ratio between the amount of fluid being lost during the injection process q_{loss} and invasion phenomena

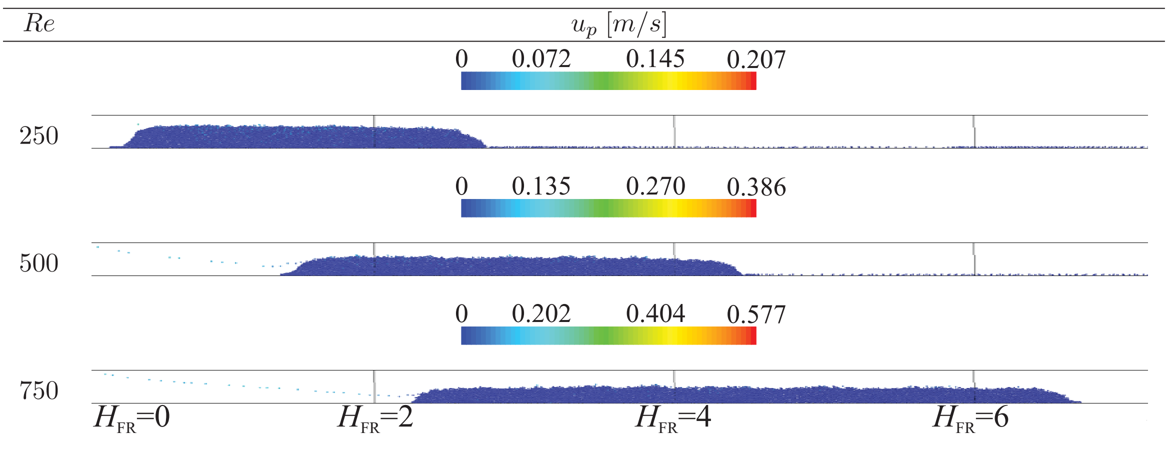

Figure 3: Particle bed inside the fracture for each Reynolds number. $\rho_{p/\beta} = 2,25$; $D_p = 0,5\ mm$

Table 2: Geometric characteristics of the particle bed for each Reynolds number

Re	$h_{pct,i}$ $[mm]$	h_{pct} $[mm]$	$e_{\%,FR}$ $[\%]$	t_{fill} $[s]$
250	15	0.108	64	76
500	64	0.135	54	90
750	102	0.196	45	136

$q_{\beta,FR,o}$, the non-dimensional fluid loss Q_{loss} is a major parameter of control, as the whole point of the technique is to reduce or eliminate the fluid loss. The monitoring of Q_{loss} is displayed in Fig 4(a).

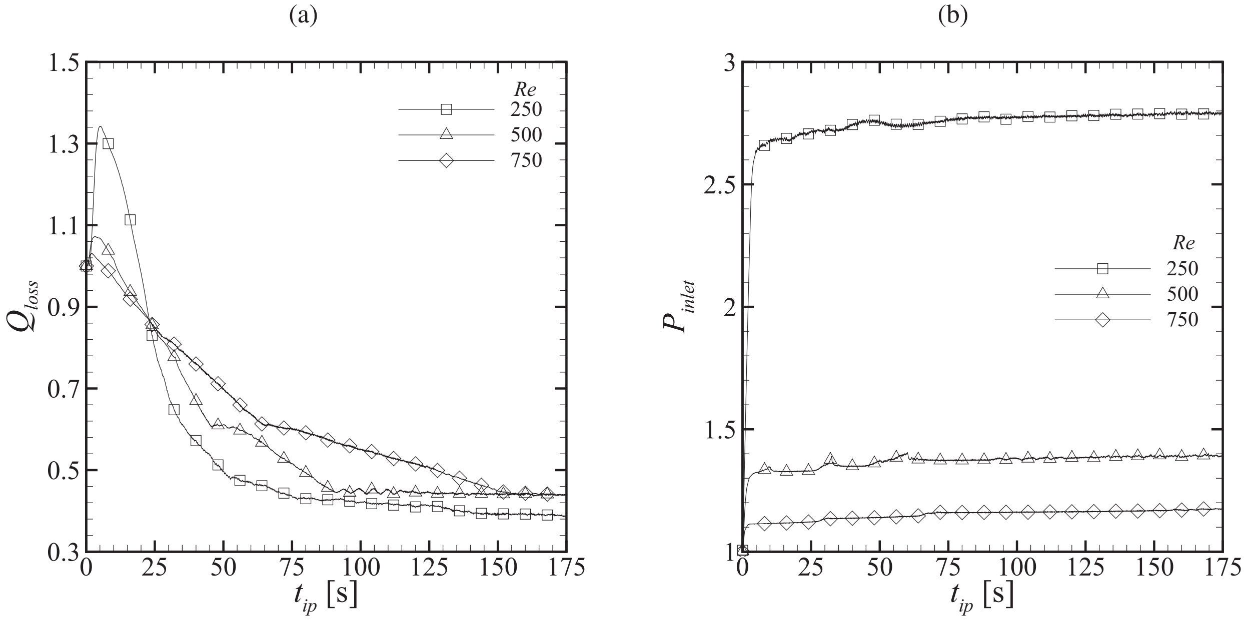

Figure 4: Monitoring of (a) Q_{loss} and (b) P_{inlet} along the time for each Reynolds number

When the particle injection process takes place, there is a related increase in the pressure on the channel inlet due to the presence of particles in the flow. Therefore, the pressure buildup P_{inlet} can be defined as the ratio between the pressure during the particle injection process $p_{m,CH,i}$ and the pressure in the loss circulation phenomenon $p_{\beta,CH,i}$, both taken in the channel inlet.

The pressure buildup monitoring can be seen in Fig. 4(b). It is possible to notice that there is an initial increase in the fluid being lost through the fracture, an event identified as overshoot. This overshoot is caused by the initial amount of particles that surpasses the fracture inlet region and do not contribute to the fracture filling process.

After the overshoot, the fluid loss through the fracture starts to decrease due to the particle packing process. The flow velocity influence the fracture filling rate, with the $Re = 250$ configuration presenting the fastest filling of the fracture $t_{fill} = 76\ s$. For $Re = 250$, the reduced fluid loss is bigger than $Re = 500$ and $Re = 750$ which are roughly the same.

As for the pressure buildup P_{inlet}, one can see that for $Re = 250$ the increase on the pressure is rather larger than for the $Re = 500$ and $Re = 750$. This can be explained by the flow velocity: as the injection process is equal for all configurations, the particle transport throughout the fracture channel is only affect by the flow velocity. Flows with small Reynolds number are more susceptible to the pressure increase due to the presence of the particles. This corroborate the overshoot hypothesis.

The next parameter evaluated is the particle to fluid density ratio $\rho_{p/\beta}$ which is related to the injections parameters. To analyze $\rho_{p/\beta}$, five values were studied, ranging from $\rho_{p/\beta} = 1.50$ to $\rho_{p/\beta} = 2.50$. To observe the filling process, the configuration of $Re = 500$ has been chosen due to its ability to carry relatively heavy particles in comparison to the $Re = 250$ and to present a significant slower flow if compared with the $Re = 750$. The fractured channel have the same geometric characteristics as described earlier.

Results for the particle packing inside the fracture, Fig 5, show that the particle to fluid density ratio strongly influence the both the length and height of the particle bed. For $\rho_{p/\beta} = 2.25$ and $\rho_{p/\beta} = 2.50$, no significant variation in the particle bed length and height is noticed, a behavior also pointed in Tab. 3, suggesting that there is an stabilization on the particle bed geometry.

Also, from Tab. 3, one can notice the significant reduction on the time t_{fill} consumed to fill the fracture. Increasing the particle to fluid density ratio provokes a decrease on t_{fill}. ExpÄžanation for that are the changes on the particle's inertia,

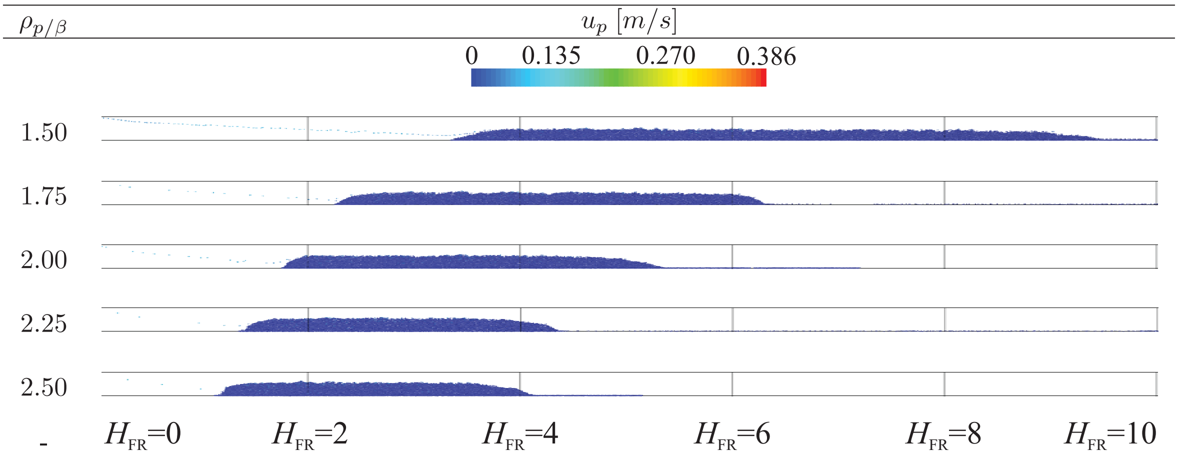

Figure 5: Particle bed inside the fracture for each Reynolds number. $Re = 500; D_p = 0,5\ mm$

which increases the particle resistance to the fluid motion, causing the particle bed to be formed closer to the fracture inlet.

Table 3: Geometric characteristics of the particle bed for each particle to fluid density ratio

$\rho_{p/f}$	$h_{i,pct}\ [mm]$	$h_{pct}\ [mm]$	$e_{pct}\ [\%]$	$t_{fill}\ [s]$
1.50	150	284	43	147
1.75	101	183	50	111
2.00	79	161	52	94
2.25	64	131	55	82
2.50	53	131	57	77

The monitoring of the fluid loss during the injection process is shown in Fig. 6(a). It is evident the difference on the time consumed to fill the fracture. Beyond that, it is possible to see that increasing $\rho_{p/\beta}$ there is an decrease of the ability of the particle bed to promote further reduction of the fluid loss Q_{loss}. This means that, although using a heavier particle promotes a faster filling of the fracture, it has the downside of diminishing the potential to reduce the fluid loss.

(a) (b)

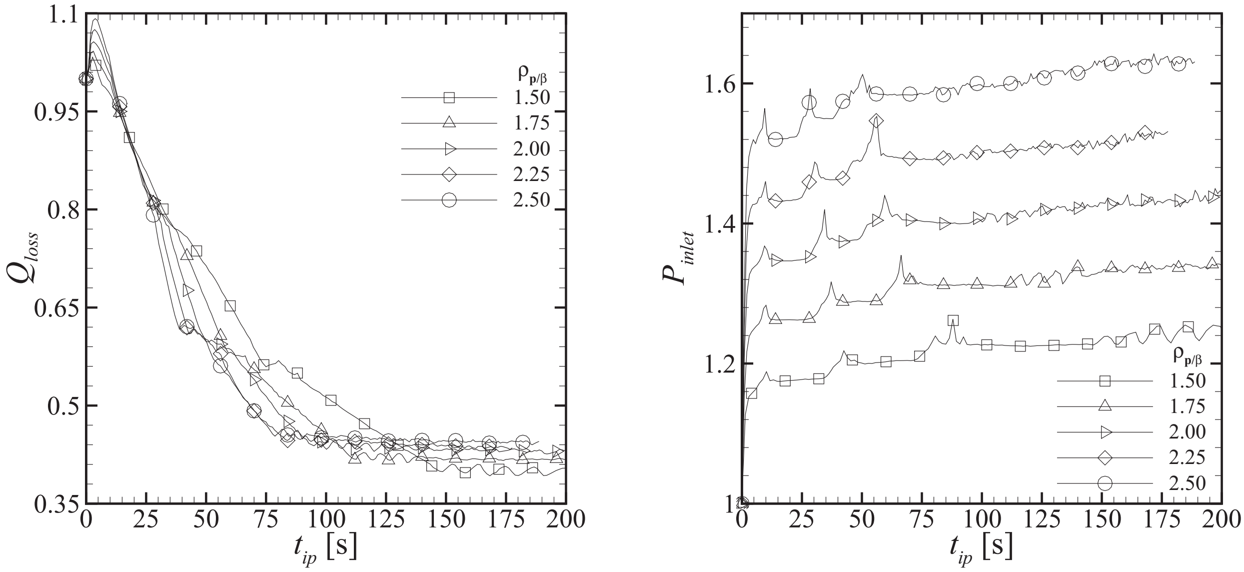

Figure 6: Monitoring of (a) Q_{loss} and (b) P_{inlet} along the time for each particle to fluid density ratio

The pressure on the fracture channel inlet is also monitored and shown in Fig. 6(b). As the mass of the particle increases, there is an increase of related pressure generated due to the particle presence which causes the respective increase of the P_{inlet}. It is crucial to monitor the pressure on the inlet channel in order to avoid the fracture pressure of the formation, as mentioned earlier.

5. FINAL REMARKS

In this work, an analysis of the lost circulation phenomenon associated with the presence of a fracture and how to address this problem was presented. The geometry of the problem was simplified using the symmetry of the wellbore and the formation was considered as an impermeable media, so the fluid loss occurs only through the fracture.

First, the lost circulation was studied by varying the flow's Reynolds number. It was observed that a higher Reynolds number tends to increase the pressure and velocity in the fracture inlet.

The next analysis focused on the filling of a fracture when the lost circulation phenomenon takes place. The technique applied consisted in adding particle of selected granulometry to the drilling fluid to form a particle bed inside the fracture, which will reduce the fluid loss.

During the injection process the influence of the flow's Reynolds number and the particle to fluid density ratio was analyzed. It was observed that using a lower Reynolds number can promote a faster filling of the fracture but has a downside of increasing the pressure in the fracture channel inlet almost 2.8x the initial one. Also, the particle bed inside the fracture can decrease in size and form itself closer to the fracture inlet when a lower Reynolds number is used.

The use of lighter particles reduces the fluid loss in a more effecive way than using heavier particles, but it increases the time required to fill the fracture. Also, the lenght of particle bed formed inside the fracture reduces when heavier particles are used, a behavior that remains until the limit of $\rho_{p/\beta} = 2.50$, for the channel and fluid conditions studied in this work.

Finally, the efficiency of the fracture filling process by injecting particles on the flow will rely on the correct combination of both the flow and the particle injection parameters.

6. ACKNOWLEDGMENTS

The authors would like to acknowledge the support of IRF/CENPES/PETROBRAS, the PRH-ANP/MCT program (PRH10-UTFPR) and the National Council for Scientific and Technological Development (CNPq).

7. REFERENCES

Barbosa, M.V., 2015. *Parametric Analysis of Particulate flow applied to sealling fractures*. Master's thesis, Federal University of Technology, Curitiba, Paraná.

Chen, Y., Yu, M., Miska, S.Z., Ozbayoglu, M.E. and Takach, N., 2014. "A novel approach in locating single loss zone during deepwater drilling with distributed temperature measurement". *Society of Petroleum Engineers*.

Cook, J., Growcock, F., Guo, Q., Hodder, M. and van Oort, E., 2012. "Stabilizing the wellbore to prevent lost circulation". *Oilfield Review*, Vol. 23, No. 4, pp. 26–35.

Crespo, F. and Ahmed, R., 2013. "A simplified surge and swab pressure model for yield power law fluids". *Journal of Petroleum Science and Engineering*, Vol. 101, No. 0, pp. 12 – 20.

De Lai, F.C., 2013. *Numerical simulation of particulated flow for filling of fractured channel*. Master's thesis, Federal University of Technology, Curitiba, Paraná.

Kendoush, A.A., Sulaymon, A.H. and Mohammed, S.A., 2007. "Experimental evaluation of the virtual mass of two solid spheres accelerating in fluids". *Experimental Thermal and Fluid Science*, Vol. 31, No. 7, pp. 813 – 823.

Li, A. and Ahmadi, G., 1992. "Dispersion and deposition of spherical particles from point sources in a turbulent channel flow". *Aerosol Science and Technology*, Vol. 16, No. 4, pp. 209–226.

Luding, S., 1998. "Collisions & contacts between two particles". In H. Herrmann, J.P. Hovi and S. Luding, eds., *Physics of Dry Granular Media*, Springer Netherlands, Vol. 350 of *NATO ASI Series*, pp. 285–304.

Morsi, S.A. and Alexander, A.J., 1972. "An investigation of particle trajectories in two-phase flow systems". *Journal of Fluid Mechanics*, Vol. 55, pp. 193–208.

Peng, Z., Zhang, X. and Dai, Q., 1996. "Leakage-plugging while drilling and plugging agents". *Journal of Central South University of Technology*, Vol. 3, No. 1, pp. 27–30.

Popoff, B. and Braun, M., 2007. "A lagrangian approach to dense particulate flows". In *Proceeding of 6th International Conference on Multiphase Flows*. Leipzig, Germany.

Suyan, K.M., Banerjee, S. and Dasgupta, D., 2007. "Practical approach for preventing lost circulation while drilling". *Society of Petroleum Engineers*.

Tiab, D. and Donaldson, E.C., 2004. *Petrophysics: Theory and Practice of Measuring Reservoir Rock and Fluid Transport Properties*. Gulf Professional Publishing.

8. RESPONSIBILITY NOTICE

The authors are the only responsible for the printed material included in this paper.